Ocean Dynamics (2015) 65:707–720
DOI 10.1007/s10236-015-0831-0

Experimental investigation on statistical properties of wave heights and crests in crossing sea conditions

Alessandro D. Sabatino[1] · **Marina Serio**[2]

Received: 7 October 2014 / Accepted: 9 March 2015 / Published online: 24 March 2015

Abstract Some theoretical and numerical studies highlighted that the occurrence of rogue waves could increase in the presence of crossing sea. This sea state is characterized by the coexistence of two wave systems with different directions of propagations and is considered one of the most common causes of ship accidents in bad weather conditions. In particular, the angle between the two interacting wavetrains, $\Delta\theta$, was found to be an important parameter that could lead to an enhanced probability of extreme events. We present an experimental investigation on wave heights and crest for surface elevation mechanically generated in different crossing sea conditions ($10° < \Delta\theta < 40°$). The results of statistical analysis confirm that the probability of extreme events increases with the angle between the two systems, but does not exceed the values of the unidirectional case, which also presents waves with greater heights. Moreover, the correlation between the heights, crests, and troughs of consecutive waves assumes higher values for the case of 40°, when compared to the unidirectional case: this could mean that it is easier to find waves of the same height within a packet in the conditions $\Delta\theta = 40°$ with respect to the unidirectional or other $\Delta\theta$ conditions considered.

Responsible Editor: Bruno Castelle

✉ Alessandro D. Sabatino
alessandro.sabatino@strath.ac.uk

[1] Marine Population Modelling Group, Department of Mathematics and Statistics, University of Strathclyde, Livingstone Tower, 26 Richmond Street, Glasgow G1 1XH, UK

[2] Dipartimento di Fisica, Università degli Studi di Torino, Via Pietro Giuria 1, 10125 Torino, Italy

Keywords Crossing seas · Rogue waves · Wave statistics · Wave correlation · Laboratory experiment

1 Introduction

The crossing sea state is characterized by the coexistence of two wave systems with different propagation directions. This state can be due to locally wind-generated waves interacting with swell (waves which travel over long distances) or of a rapidly turning wind (in this case waves may have similar frequencies) and is quite common in seas. For example, analysis of the occurrence of crossing sea conditions in the North Atlantic Ocean shows that this condition occurs, on average, in 22 % of the recorded cases (Guedes Soares 1984). Subsequent analysis shows that the mixed sea state occurs about 25 % of the time in both coastal and open sea (Guedes Soares 1991).

In last few years, there was a rising interest on this particular state since the crossing sea has been appointed in the last years as one of the factors responsible for rogue wave occurrence (Onorato et al. 2005, 2006, 2009a; Zakharov et al. 2006).

Rogue waves, sometimes called monster waves or freak waves, are a major threat to the marine transportation system. At least 22 supercarriers have been lost because of rogue waves between 1969 and 1994 all around the world (Kharif and Pelinovsky 2003). Moreover, several studies highlight that rogue waves can be a serious threat for marine structures, such as oil platforms (Haver 2004; Nikolkina and Didenkulova 2011; Bitner-Gregersen and Toffoli 2014). It is generally accepted that a wave can be defined "rogue" when its height exceeds twice the significant wave height of the ocean in which was generated. An alternative definition can be also found in Dysthe et al. (2008) in which a rogue wave is defined as a wave whose crest is more than 1.25 times the significant wave height. Extensive reviews of the theoretical

and laboratory experiments on freak waves carried out in the last years can be found in Muller et al. (2005), Akmediev and Pelinovsky (2010), Onorato et al. (2013).

In deep water, that is the conditions in which our experiment was carried out, there are generally four causes for the formation of rogue waves: wave-current interaction (Gründlingh 1994; White and Fornberg 1998; Lavrenov 1998, 2003), modulational instability (Onorato et al. 2001; Galchenko et al. 2010, 2012), dispersive (or linear) focusing (Bona and Saut 1993; Magnusson et al. 1999; Pelinovsky et al. 2001), and a crossing sea state (Donelan and Magnusson 2005; Gramstad and Trulsen 2010).

In the present paper, we investigate the formation of rogue waves in a crossing sea due to modulational instability. Modulational instability, or Benjamin-Feir instability, is described by the Nonlinear Schrodinger equation (NLS) and is due to side-band perturbations in a uniform narrow banded wave train. A review on the studies appointed in the past on this mechanism, that is extremely important in very different fields such as electrodynamics, nonlinear optics, hydrodynamics and quantum mechanics, can be found in Zakharov and Ostrovsky (2009). Onorato et al. (2006) proposed that the modulational instability could be a suitable mechanism for explaining the formation of rogue waves in a crossing sea. They studied the crossing sea state with a system of Coupled Nonlinear Schrodinger (CNLS) equations, defining a dispersion relation in which the first term was the Benjamin-Feir index (BFI), that is the ratio between nonlinearity and dispersion, which is of great importance for the modulational instability in unidirectional sea.

In Toffoli et al. (2006), second-order simulations show that there is an increase of the probability for extreme waves in crossing seas. Using a system of CNLS equations for simulating a crossing sea, Onorato et al. (2010) found that most probable angles for establishing a rogue wave are $\Delta\theta<35°$, since the nonlinear and dispersive terms in CNLS equations have the same sign (the system is focusing) and their ratio become larger with $\Delta\theta$ approaching 35°. A successive experiment on the same wave tank used for this study found that the kurtosis in this particular state of the sea increases with the crossing angle $\Delta\theta$ (Toffoli et al. 2011). The kurtosis is a fundamental parameter directly linked to the nonlinearities of the wave train, in particular with the Benjamin-Feir index, and to the rogue wave probability for unidirectional sea state (see e.g., Benjamin and Feir 1967; Janssen 2003; Cherneva and Guedes Soares 2011).

Roberts (1983), computing steadily propagating short-crested due to the nonlinear interaction between two wave trains, using Padé approximants, found that in a directional sea, higher wave crests are expected for values of crossing sea angle in the range of $25°<\Delta\theta<55°$. An enhanced probability of freak waves was found by Gramstad and Trulsen (2010), using numerical Monte-Carlo simulations, when a wave train interacts with a system of swell waves. In particular, the highest probability for the establishment of rogue waves was found for $\Delta\theta=45°$.

Also, some field measurement confirmed the hypothesis that crossing seas could lead to an enhanced probability of the formation of rogue waves, with respect to the classical theory. In particular, the crossing sea was found to be responsible for some accidents that occurred during the last years. Greenslade (2001) studied the conditions of the 2008 Sydney-Hobart race, that was defined as one of the most disastrous yacht race that ever occurred (5 yachts were forced to retire and the other 66 boats followed the same destiny): during the peak storm, in the sea were present two wave systems. Cavaleri et al. (2012) examined the Louis Majesty accident, provoked by a large wave that hit the 207-m large ship, destroyed some windows, and caused two fatalities. Studying the weather and the sea condition of that day, the authors concluded that this accident happened in crossing sea condition, characterized by two wave systems with similar frequencies.

The aim of this study is to examine the behavior of extreme wave probability in a wave tank crossing sea condition ($10°<\Delta\theta<40°$, $\Delta\theta$ is the angle between the two wave systems) and its evolution trough the wave tank. The spatial evolution of main variables is a very important indicator for the modulational instability occurrence: a previous experiment carried out for unidirectional waves highlighted an increase of the kurtosis during the propagation, with a maximum for $x/L>20$, where L is the wavelength of the wave train (Onorato et al. 2005). We also compared the rogue wave probability between a crossing sea state and unidirectional wave field, and we investigated the agreement between theoretical distribution of wave crests and wave heights (Tayfun 1980; Socquet-Juglard et al. 2005) and experimental laboratory data for the crossing sea, to complement the investigation carried out for unidirectional case (Onorato et al. 2005) and presence of spreading.

Another interesting parameter is the correlation coefficient for successive wave heights, crests, and troughs that is strictly connected to the wave group theory. A wave group is a sequence of waves whose heights exceed a certain threshold (Rodríguez and Guedes Soares 2001), and it can represent a threat on marine infrastructures and marine transportation. So from the engineering point of view, predicting its features is fundamental.

The correlation is a key factor in the grouping theory: the Markov process theory proposed by Kimura concludes that the wave grouping, in particular the length of a wave group, is strongly dependent on the structure of the sea state, and can be measured by the correlation coefficient between consecutive wave heights (Kimura 1980; Longuet-Higgins 1984). Successive studies have confirmed this theory and is valid in different cases, such as mixed sea state (Sobey 1996; Rodríguez et al. 2000).

Wave heights correlation has been studied in wave growth and decay state (Rye 1974; Su et al. 1982), in Pierson-

Moskowitz conditions (Arhan and Ezraty 1978; Rodríguez and Guedes Soares 2001; Sobey 1996), JONSWAP (Arhan and Ezraty 1978; Sobey 1996), in swell waves (Goda 1983), and in other different conditions (Dattatri et al. 1977; Wist et al. 2004), finding quite different values for each condition. Crossing sea state correlation coefficient, in JONSWAP conditions, are not completely studied. Numerical simulations based on Pierson-Moskowitz spectrum have highlighted, however, that the crossing sea have an increased value of the successive wave heights correlation coefficient compared to the unidirectional case (Rodríguez and Guedes Soares 2001).

Although successive wave height correlation was studied in different conditions, a laboratory experiment is crucial to confirm both theoretical and numerical studies and to understand if the correlation coefficient depends or not on the crossing sea angle and to compare the previous findings.

The paper is organized as follows. In § 2, we describe the facilities used for the experiments and the different wavefields considered. The resulting statistical properties of the surface elevation, wave heights, and wave crests are reported in § 3. The correlation of heights, crests, and troughs is discussed in § 4; conclusions are then included in § 5.

2 Experimental set-up

The experiments have been performed at the MARINTEK wave facilities in Trondheim, Norway. Waves have been generated in a three-dimensional wave tank, with dimensions 70 m×50 m, one of the largest in the world.

The basin is fitted with two sets of wavemakers. Along the 50-m side, there is a double flap, hydraulically operated unit for generating long-crested, regular, and irregular waves. The second wavemaker (the one used for present tests) is fitted along the 70-m side of the basin. It consists of altogether 144 individually computer-controlled flaps. This unit can generate short-crested seas within a wide range of directional distributions of the wave energy. The basin is equipped with a system that is capable of changing the water depth: for the present experiment, the water depth was fixed at 3 m. The wave basin is also equipped with two minimum-reflection beaches: one is located in front of the directional wavemaker, while a second one is on the right-hand 50-m side. For the present study, we used data from nine wave gauges aligned perpendicular to the wavemaker, with 5-m equidistance, in the central area of basin (for details see Onorato et al. 2009a, b).

From the theoretical point of view, the modulational instability in crossing seas has been studied using a system of coupled NLS equations, therefore to test the numerical conclusions, irregular waves were mechanically generated according to an input spectrum composed by the sum of two identical JONSWAP spectra (Komen et al. 1994) describing two long-crested wave fields, propagating along two different directions, with the energy distributed only in frequency and not in angle. Each spectrum has a peak period T_p=1 s, which corresponds to a peak wave length λ_p=1.56 m, a significant wave height H_s=0.068 m, and a peak enhancement factor γ=6; the wave steepness is $k_p a$=0.14, where k_p is the wavenumber at the spectral peak and $a=H_s/2$. Complex Fourier amplitudes are randomly chosen around the target JONSWAP spectrum, and the random phases are assumed to be uniformly distributed in the interval [0, 2π]. The systems were forced to propagate along two different directions, which are symmetrical with respect to the normal to wavemaker. The following angles between the two systems were considered: Δθ= 10°, 20°, 30°, and 40°.

The peaks were generated in order to maintain the directional spreading constant for all the experiment and narrow. The spreading was evaluated using the method reported in Donelan et al. (1996). The result of this analysis is reported in Toffoli et al. (2011).

Surface elevation was recorded with a sampling frequency of 80 Hz: about 4500 individual waves were measured at every probe for each value of Δθ. We analyzed also the data recorded during the same experimental sessions, characterized by a single JONSWAP spectrum, in order to compare the results of a crossing sea with unidirectional wave fields.

3 Amplitude, height, and crests statistical behavior

In Fig. 1, we present, for the various value of Δθ, the probability density function of the surface elevation at different distances from the wavemaker divided by the wavelength corresponding to the peak of the spectrum at the first probe L. For convenience, we scale the surface elevation by the standard deviation σ of the concurrent time series. The experimental probability density function is compared to the Gaussian distribution and to the following second-order distribution

$$p(\eta) = \frac{1-7\sigma^2 k_p^2/8}{\sqrt{2\pi\left(1+3G+2G^2\right)}} \exp\left(-\frac{G^2}{2\sigma^2 k_p^2}\right) \qquad (3.1)$$
$$G = \sqrt{1+2\sigma\eta k_p^2} - 1$$

The second-order theory (Longuet-Higgins 1963) is the general description of the surface elevation that takes into account bound modes up to second order in wave steepness. Tayfun (1980) derived a formula for the distribution of wave crests in the narrow-band approximation, for infinite water depth and under the hypothesis that free waves are described

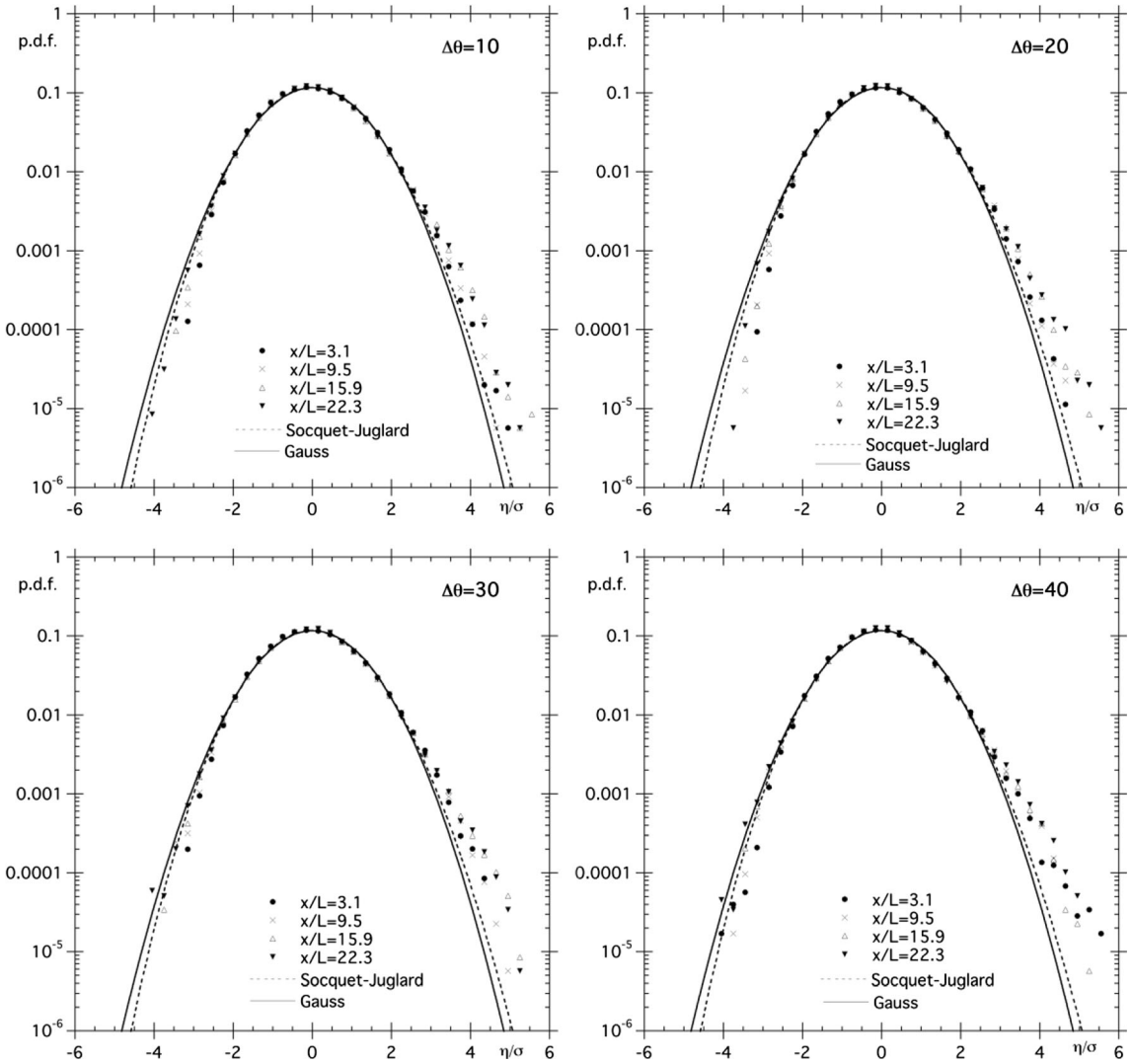

Fig. 1 Probability density function of surface elevation for the four crossed sea configurations. *Dashed line*: Equation (3.1), Socquet-Juglard distribution. *Solid line*: Gaussian distribution

by a Gaussian statistics. Relation (3.1) has been derived in Socquet-Juglard et al. (2005) as an approximation of the Tayfun second-order distribution and is used here as a term of comparison for experimental statistical behavior.

It may be noted that while the waves propagate in the tank, there is an increasingly significant deviation of the upper tail of the probability density function from the Tayfun distribution. This result is expected and already widely tested in previous experiments (see Onorato et al. 2013 for a detailed report and discussion). This behavior occurred for all values of $\Delta\theta$, with no significant differences between the four configurations.

The deviation in the upper tail may be best investigated through the statistical parameters of higher order, skewness, and kurtosis. In particular, the kurtosis is considered a measure of the probability of occurrence of extreme waves. In order to give an estimate of the skewness and kurtosis, we consider the narrow-banded approximation of the second-order theory: for deep water waves, the skewness (λ_3) and kurtosis (λ_4) take the following form (Janssen 2009)

$$\begin{aligned}\lambda_3 &= 3\left(\sigma k_\mathrm{p}\right)\\ \lambda_4 &= 3 + 18\left(\sigma k_\mathrm{p}\right)^2\end{aligned} \tag{3.2}$$

where k_p is the wavenumber at the spectral peak and σ is the standard deviation. For our data, k_p and σ are estimated at each probe for every crossing sea configuration. The spectral peak was evaluated using a method proposed by Young (1995) that found that the most robust estimator for the peak period is:

$$f_p = \frac{\int_0^\infty f \cdot P^4(f)\,df}{\int_0^\infty P^4(f)\,df} \tag{3.3}$$

where power spectra are determined by splitting the series into segments of 8192 points and calculating the moving average of the subseries spectra.

In Fig. 2, we report the spatial evolution of standard deviation and spectral peak frequency: while σ varies non-monotonically along the basin, there is a clear downshift of the peak frequency. The percentage decrease depends on angle between wave trains, varying from 5.2 % for $\Delta\theta=10°$ to 3.3 % for $\Delta\theta=40°$.

Figure 3 shows experimental values of the skewness (panel a) and kurtosis (panel b) along the wave basin compared with theoretical values calculated with (3.2) error bars for theoretical values that take into account the variability of the peak frequency and standard deviation for each crossing sea configuration, while experimental values have statistical error of the order of 0.02, too low for graphical limits. The behavior of the two parameters is different. The skewness λ_3 always overestimates the experimental values, which does not suggest a particular angle dependence. For the fourth order moment, the kurtosis almost monotonically increases as the waves propagate along the basin and increases with the angle between the two wave systems. Moreover, from $x/L=13$, the value of λ_4 underestimates the experimental values up to 12 % for $\Delta\theta=40°$. Toffoli et al. (2011) compared these experimental results with numerical simulations of a third order truncation of the potential Euler equations, which confirm the increase of kurtosis and suggest that the maximum value is achieved for $40° < \Delta\theta < 60°$. Onorato et al. (2010) studied the modulational instability for two equal, noncollinear wave systems traveling at angle θ: in particular, they investigated the dependence of growth rate and amplification factor from θ. Their analysis indicates that extreme waves may appear with a higher probability for an angle between 10 and 30°.

Therefore, our attention moves to the height of the waves, herein denoted by H, and the wave crest η_c. In the study of extreme events, it is useful to define the probability that the wave height H assume a value larger than a reference height, H_0. This probability, also known as the survival function $S(H>H_0)$, is given by $1-P(H\le H_0)$, where P is the cumulative probability function. Longuet-Higgins (1952) showed that if the wave spectrum is narrow banded and if the phases of the Fourier components of the surface elevation are randomly distributed, then the probability distribution of wave heights, crests, and troughs is given by the Rayleigh distribution. For the Rayleigh distribution, which holds for second-order theory, the survival function is given by

$$S(H/H_s > H_0/H_s) = \exp\left[-2\cdot(H_0/H_s)^2\right] \tag{3.4}$$

where H_s is the significant wave height, normally identified with 4σ.

Figure 4 shows the experimental survival function at four different positions in the wave basin, compared with the Rayleigh distribution (3.4). It can be seen that for distances from wavemaker lower than 16 L, the frequency of wave heights falls below the limit of the Rayleigh distribution: only for the case $\Delta\theta=40°$ and $x/L=15.9$, the experimental tail is superimposed on the theoretical one. For greater distances, the frequency of waves with $H>1.5H_s$ is greater than that expected from the Rayleigh distribution, except for $\Delta\theta=10°$.

The survival function for wave crests η_c, as derived from the Tayfun distribution, is given by

$$S[(\eta_c/H_s) > (\eta_0/H_s)] = \exp\left\{-\frac{8}{(k_pH_s)^2}\left[\sqrt{1+2(k_pH_s)\frac{\eta_0}{H_s}}-1\right]^2\right\} \tag{3.5}$$

where k_p is the dominant wavenumber. The Tayfun formula enhances the tail of the Rayleigh distribution, especially if the wave steepness is large. The departure from the Rayleigh distribution is due to the presence of bound (phase locked) modes and not to the dynamics of free waves. This means that the Stokes wave nonlinearity is accounted for, but the nonlinear interactions among free wave components are not.

Figure 5 shows the experimental survival function at four different positions in the wave basin. In each panel, we compare the function for the different crossing sea configuration with the Tayfun distribution (3.5), where the values of peak

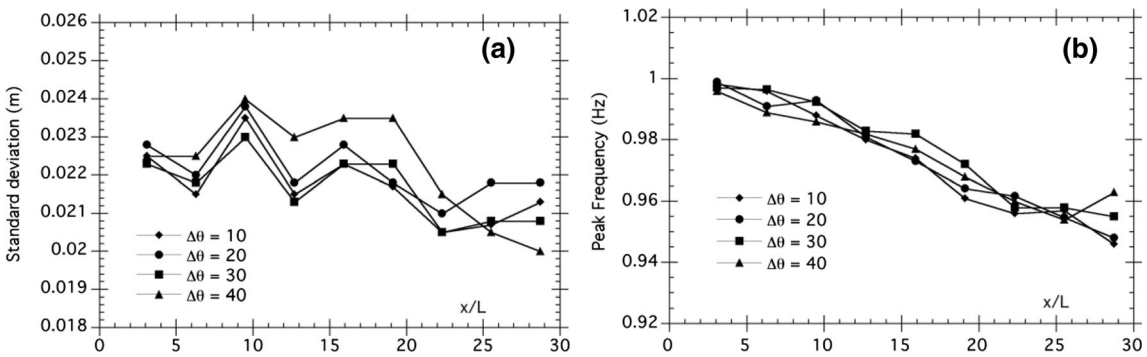

Fig. 2 Evolution as a function of distance from the wavemaker. **a** standard deviation. **b** peak frequency

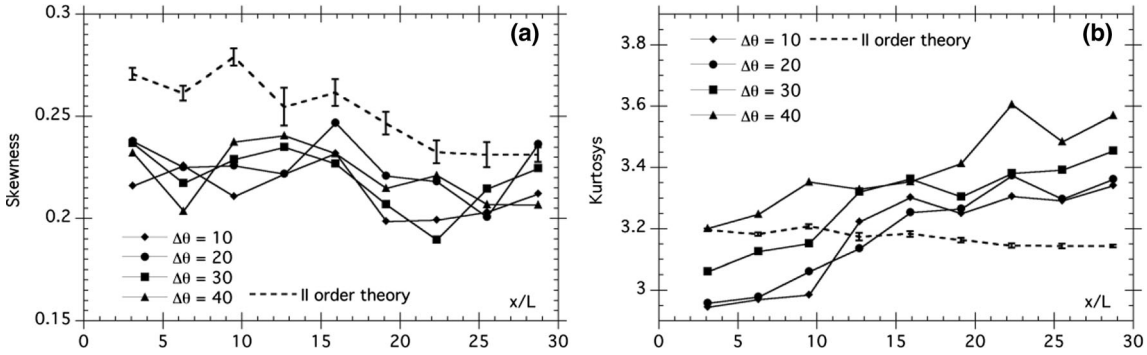

Fig. 3 Spatial evolution as a function of distance from the wavemaker. **a** skewness. **b** kurtosis. *Dashed lines* represent expected values calculated from (3.2); *error bars* take into account the variability of the peak frequency and standard deviation for each crossing sea configuration

frequency and standard deviation for each sea state are evaluated on the whole series. For distances from wavemaker $x/L \leq 10$ (with the exception of 40° and $x/L=3.1$, due to large crests recorded close to the generator), the second-order theory provides a good estimate of the experimental data, while for greater distances Tayfun function slightly underestimate the experimental probability for $\eta_c/H_s \geq 0.8$. Toward the end of the basin, $x/L=28.7$, the crest amplitude attenuates, and so the deviation from second-order theory. The behavior shows no significant dependence on the value of $\Delta\theta$. It is interesting to relate Figure 4 to Figure 16 in Onorato et al. (2009b), relative to irregular, unidirectional waves recorded in the same experimental session. At $x/L=3.1$, the survival function is almost comparable for crossing and unidirectional sea, but for $x/L=15.9$ crossing sea distribution is more similar to unidirectional case A.

Mori et al. (2007) discuss the need to establish a distribution of maximum wave height, and not only of the height in general, to improve the prediction of extreme waves. They refer to Modified Edgeworth Rayleigh (MER) distribution

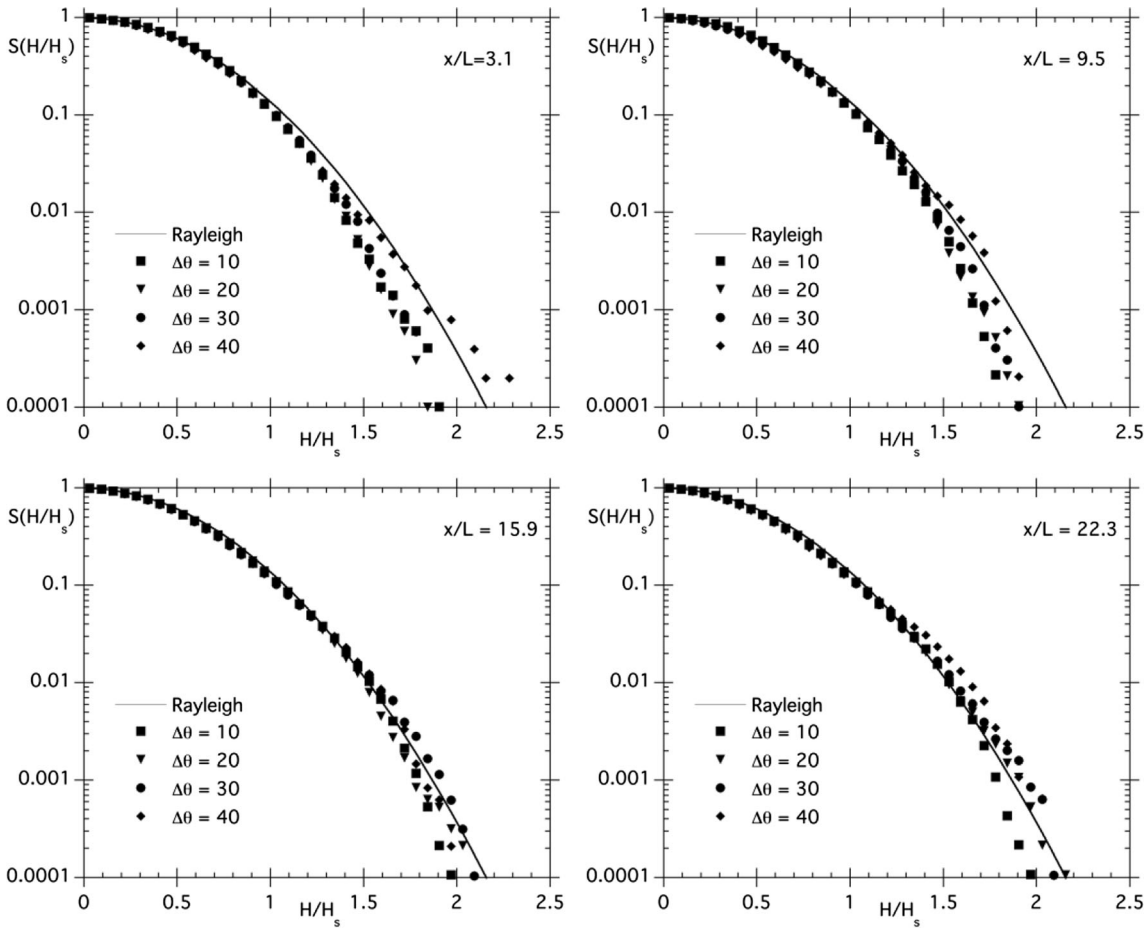

Fig. 4 Wave height survival function for crossing seas at different distances from the wavemaker. *Solid line* corresponds to the Rayleigh distribution

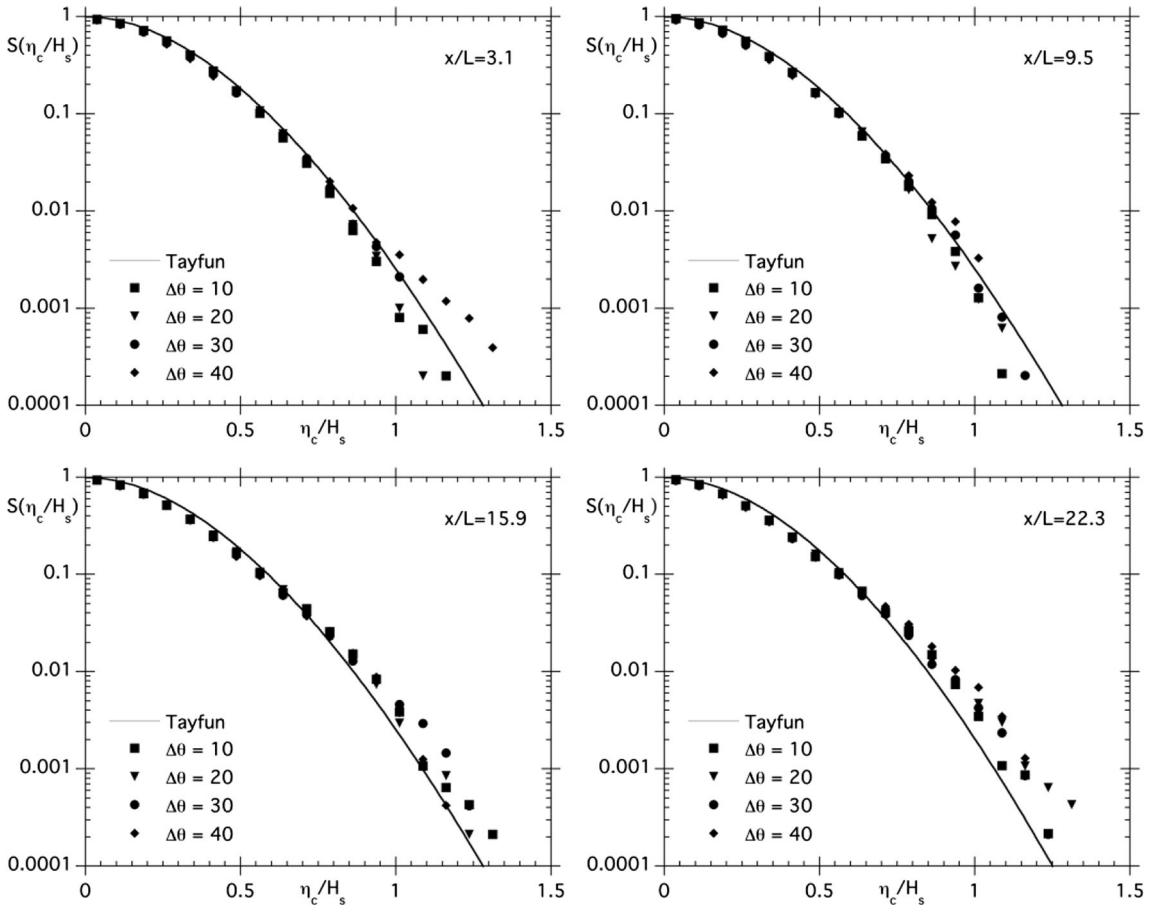

Fig. 5 Wave crest survival function for crossing seas at different distances from the wavemaker. *Solid line* corresponds to the Tayfun distribution

(Mori and Janssen 2006) whose main limitation is that nonlinear effects are included in the distribution via the kurtosis, which requires a large number of data to converge. We use the procedure to derive the experimental distribution of the maximum heights, by directly comparing crossing toward unidirectional configuration. We divide wave height series in segments of 150 waves, and we extract the maximum height in each segment, obtaining sets of around 40 values of H_{max} for every $\Delta\theta$.

Figure 6 reports the experimental distribution of H_{max} at four different distances from the wavemaker. One can see that the distribution for the various $\Delta\theta$ initially overlaps with the unidirectional case. Then, with the propagation, the unidirectional distribution moves to maximum heights greater than those of the crossing sea cases. The average H_{max} increases around 10–12 % for crossing cases and 15 % for unidirectional one: this increase is statistically significant ($p<10^{-5}$). On the other hand, there is not a significant difference in behavior as a function of $\Delta\theta$, probably due to the low statistics.

Similar considerations come from the analysis of highest waves characteristics for each configuration. Figure 7a show the maximum wave height recorded at each probe for all the experimental data sets. For most distances, the highest wave is recorded in unidirectional case while three probes recorded the maximum height for $\Delta\theta=40$. One of these cases concerns the probes closer to the wavemaker, for which the modulational instability cannot be regarded as relevant in the formation of rogue waves. It is not possible to establish a relationship between H_{max} and $\Delta\theta$ consistent for the entire basin, since for the first probes ($x/L<10$) H_{max} increase with $\Delta\theta$, while at greater distances the trend seems to be more erratic.

If we define an extreme wave as a wave such that $H>8\sigma$, we can evaluate the extreme wave frequency, that is the number of extreme waves normalized to total number of wave, presented in Fig. 7b. The frequency grows during propagation, but in five out of nine probes the value relative to $\Delta\theta=40°$ is higher than the unidirectional one and is always lower than $5\ 10^{-4}$ for $\Delta\theta=30°$. The total frequency over the entire basin for $\Delta\theta=40°$ is comparable to that of the unidirectional case, and is greater than that of other $\Delta\theta$ values. So we can say that a greater number of extreme waves may occur with the growth of the angle between the two wave trains, with a height value that approaches the unidirectional ones.

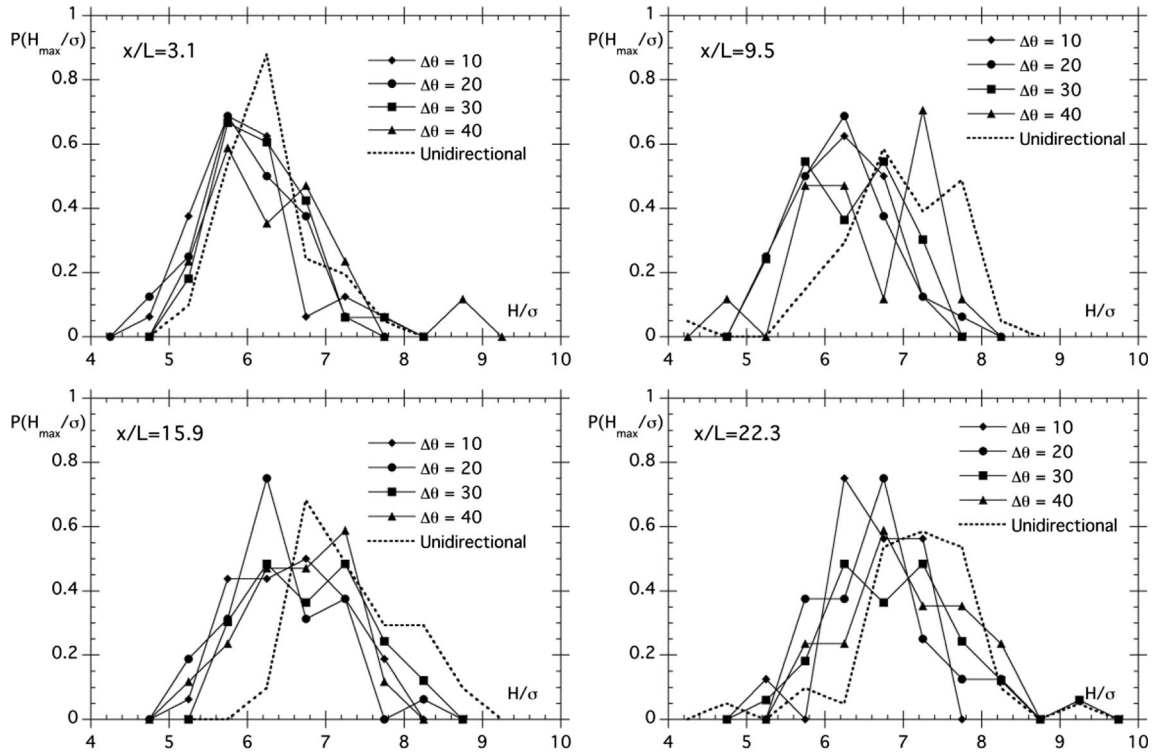

Fig. 6 Maximum wave height distribution for crossing and unidirectional seas at different distances from the wavemaker

4 Correlation of heights, crests, and troughs

The Markov wave group theory, formulated by Kimura (1980), assumes that successive wave heights are correlated. From this assumption, he considered time series of wave heights as a two-state Markov chain. These two states are determined by the exceedance or the non-exceedance of a given height threshold H_0.

From this wave group theory, and from the assumption that wave heights follows a Rayleigh distribution, Kimura manages to build a joint distribution of successive wave heights H_1 and H_2, given by

$$p(H_1,H_2)=\frac{H_1H_2}{(1-\kappa^2)16m_0^2}\exp\left[-\frac{H_1^2+H_2^2}{(1-\kappa^2)8m_0}\right]I_0\left[\frac{H_1H_2\kappa}{(1-\kappa^2)4m_0}\right]$$

where m_n are the spectral moment of order n, I_0 is the modified Bessel function of order zero, and κ is a correlation factor that is given by (Rodríguez and Guedes Soares 2001):

$$\kappa(\tau)=\left[\frac{1}{m_0^2}\left(\left(\int_0^\infty S(f)\cos(2\pi f\tau)df\right)^2+\left(\int_0^\infty S(f)\sin(2\pi f\tau)df\right)^2\right)\right]^{1/2}$$

with $\tau\approx T_{02}$, that is the average zero-crossing period estimated from the spectra and given by $T_{02}=(m_0/m_2)^{1/2}$. The correlation factor is related to the correlation coefficient between successive wave heights:

$$R_{HH}=\frac{E(\kappa)-\frac{1}{2}(1-\kappa^2)K(\kappa)-\frac{\pi}{4}}{1-\frac{\pi}{4}}$$

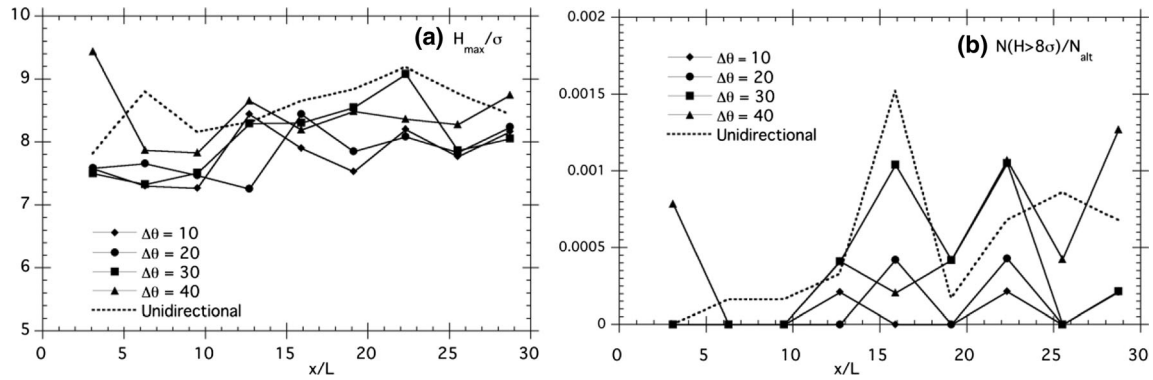

Fig. 7 **a** Maximum wave height recorded at each probe. **b** Extreme wave frequency

where the two function E and K are, respectively, the complete Jacobian elliptic integrals of the first and the second kind. An approximate relation of the R_{HH} is given by:

$$R_{HH} = \frac{\pi}{16-4\pi}\left(\kappa^2 + \frac{\kappa^4}{16} + \frac{\kappa^6}{64}\right)$$

From the Kimura theory, it is clear that a higher correlation coefficient means that the wave grouping is higher: given a certain threshold, H_c, the probability that two successive wave heights are both higher than this value is given by:

$$p_{22} = \frac{\int_{H_C}^{\infty}\int_{H_C}^{\infty} p(H_1,H_2)\,dH}{\int_{H_C}^{\infty} p(H)\,dH}$$

The degree of dependence between successive wave heights (H), crests (C), and troughs (T) is examined through the correlation coefficient. The correlation coefficient is calculated for every angle as an average performed on all the wave gauges, and we associate the standard error as uncertainly to the measure. We studied correlation between wave i and wave $i+1$ ($R_{(1)}$), wave ($i+2$) ($R_{(2)}$), wave ($i+3$) ($R_{(3)}$), and wave ($i+4$) ($R_{(4)}$).

In Fig. 8, we reported the spatial evolution of $R_{HH(1)}$ and $R_{HH(2)}$: the correlation coefficient is quite stable along the wave tank, showing no significant propagation effect. Relative errors (evaluated from standard error) range from 0.006 to 0.016 for $R_{HH(1)}$ and from 0.02 to 0.10 for $R_{HH(2)}$.

Figure 9a shows the values obtained for correlation $R_{HH(1)}$ and $R_{HH(2)}$ with an average over the distance from wavemaker: in all case, the correlation has a minimum for $\Delta\theta=10°$ and increases with angle. Note that the maximum occurs for $\Delta\theta=40°$, with a value larger than unidirectional one from 10 % for $R_{HH(1)}$ to 80 % for $R_{HH(2)}$: the same results hold for crests and troughs. In Fig. 9b, we report correlation coefficients $R_{HH(i)}$ ($i=1.4$) for $\Delta\theta=40°$ and unidirectional waves, and the last ones are always lower than the crossing sea case, but with a gradually decreasing difference. Wist et al. (2004) reported in Figure 13a similar behavior for different $R_{HH(i)}$ for observed wave data both in nature and in the laboratory.

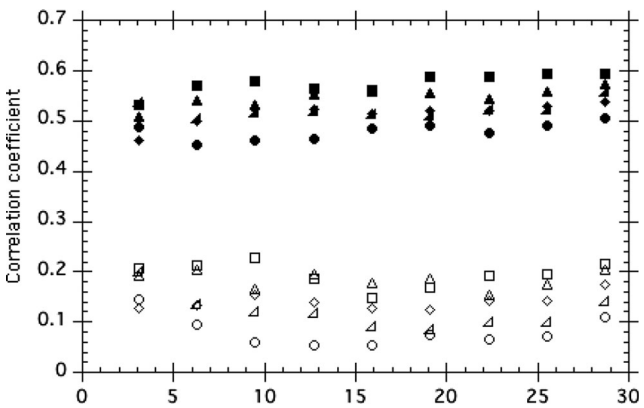

Fig. 8 Correlation coefficients for successive wave heights at different distances from the wavemaker: *black lower right triangle* (unidirectional), *black circle* (10°), *black diamond* (20°), *black triangle* (30°), *black square* (40°). *Full symbols* corresponds to $R_{HH(1)}$, *empty symbols* to $R_{HH(2)}$

We compare in Table 1 our results for heights with previous studies, integrating those reported in Rodríguez and Guedes Soares (2001, see Tables 3 and 4—R-GS in the following), which include both experimental and numerical simulation data.

It can be observed that correlation coefficients for the MARI NTEK experiment, both for crossing and unidirectional configurations, are among the highest compared to those reported in the literature. They are similar to those obtained for a long-traveled swell (Goda 1983), for a peaked JONSWAP spectrum (Sobey 1996), for wind-sea-dominated mixed sea state (R-GS), and for long-crested wave—JONSWAP spectrum in wave tank (Wist et al. 2004). In particular, the comparison with R-GS is important, which observed that the correlation between successive heights mainly increases for wind-sea-dominated sea states and large intermodal distance (spectral peak frequency separation). They have pointed that often wind-sea states coexist with a background swell, having small energy contents and short peak frequency: as a consequence of correlation growth, this situation is characterized by an increasing probability of successive large wave height (wave group). In our case, however, the frequencies of the two systems are equal and similar is the energy content. It is also interesting to note that correlation becomes negative for [i,i+4], as in R-GS states *I* (swell and wind-sea spectral peaks very near to each other) and *c* (mixed wind-sea and swell systems with comparable energy).

Then, we could argue that the presence of two wave trains with different directions of propagations increases considerably the correlation between consecutive wave heights and accordingly the amount of wave grouping. Furthermore, the increase is proportional to the angle between the two wave trains and overcomes the unidirectional value for $\Delta\theta>20°$.

In Table 2, we show the computed correlation coefficients for the wave crests and troughs. Results clearly shows that the correlation coefficients for these variables are angle dependent, as also shown by Fig. 8a, furthermore the values are lower than those found for heights.

These results require further studies, with the analysis of the joint distributions of successive wave's heights and crests, and of the closely related conditional distribution, as well as the analysis of period distributions and correlation.

5 Discussion and conclusions

We have presented the statistical analysis of wave heights and crest for surface elevation mechanically generated in different crossing sea conditions ($10°\leq\Delta\theta\leq40°$).

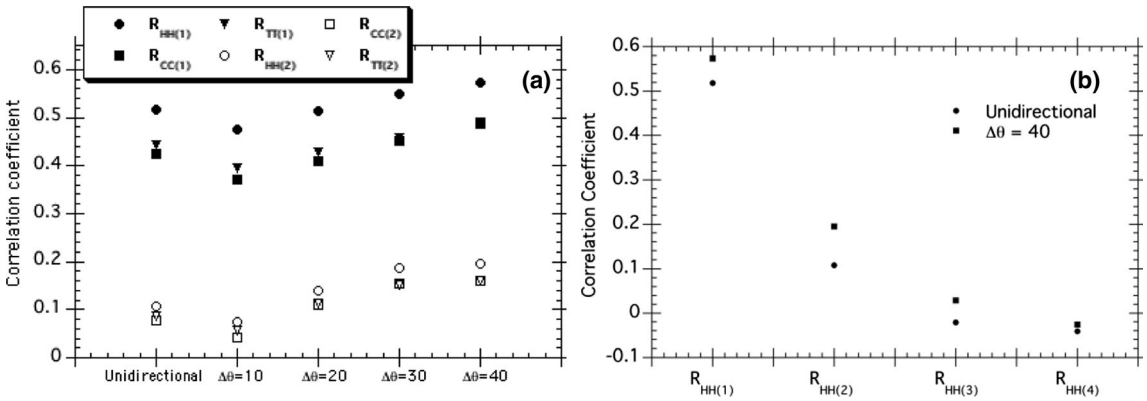

Fig. 9 **a** Correlation coefficients $R_{(i)}$ (i=1.2) for successive wave heights, crests, and troughs. **b** Correlation coefficients $R_{HH(i)}$ (i=1.4) for $\Delta\theta = 40°$ and unidirectional waves

The results highlight that the probability of extreme events increases with the angle between the two systems, but does not exceed the values of the unidirectional case, which also presents waves with greater heights.

Onorato et al. (2010), studying the dependence of the grow rate and amplification factor from the angle θ, have found that freak waves may appear with a higher probability for angles between 10 and 30°: this range is characterized by large and simultaneous values of amplification factor and grow rate, with a theoretical limit at 35.264°, for which the dispersion is minimum. Our results show an increase in the probability of extreme waves up to 40°, not showing a statistically different behavior between $\Delta\theta$=30° and $\Delta\theta$=40°, experimentally confirming the results from previous numerical simulations using Potential Euler equation (Toffoli et al. 2011).

Moreover, we confirm the monotonically increase of kurtosis as the waves propagate along the basin and with the angle between the two wave systems (obtained from numerical simulation by Onorato et al. 2010—see Fig. 7), underestimated by narrow-banded approximation of the second-order theory for the most part of the basin. It is also interesting to note that our experiment highlight that the unidirectional case presents higher maximum wave heights rather than the crossing sea case.

The growth of kurtosis along the basin is in agreement with the modulational instability mechanism, and the evolution of kurtosis in the crossing sea was similar to the one found in experiments carried out in unidirectional sea state, such as Onorato et al. (2005). The increase of this statistical parameter during the propagation of the wave train in the crossing sea was also predicted by previous numerical simulations in unidirectional sea state (Mori et al. 2011), that highlighted also that the directional dispersion of the spectrum poses a limit for the growing of the kurtosis.

Gramstad and Trulsen (2007) and Onorato et al. (2002) discovered from numerical experiment that the directionality of the spectrum, in particular its directional spreading, prevent the formation of rogue waves in a sea state in which only one frequency peak was present. This numerical result was confirmed by two independent wave tank experiments, carried out in MARINTEK and in Tokyo wave basin (Onorato et al. 2009a) and by another experiment with different initial directional spreading and BFI values (Onorato et al. 2009b). However, it is still not clear how in crossing seas the interaction with two different wave trains with two different directional spreading and two different directions could affect the rogue wave frequency. Field measurements and numerical simulations carried out recently in crossing seas conditions, however, suggests that the effect of the directional spreading on the rogue wave probability is weaker than in unidirectional seas (see in particular Christou and Ewans 2011; Bitner-Gregersen and Toffoli 2014): both of these papers lead to the conclusion that rogue waves occurs also for broad-banded spectra. In particular, Bitner-Gregersen and Toffoli (2014) concluded that the maximum kurtosis occurs for 40°, independently on the directional spreading, suggesting that both rogue waves probability and maximum wave height are strongly dependent on the crossing sea angle rather than directional spreading.

The present experiment was carried out maintaining a low directional spreading (for more details about the dispersion of this experiment see Toffoli et al. 2011), in order to study the case of a focusing of the wave train and to minimize the dispersive term in the Benjamin-Feir instability. This low directional spreading was evaluated near the absorbing beach using a wavelet directional method (Donelan et al. 1996). The directional spreading was constant for both wave train and for all the experiment, in order to study the crossing sea state in the same condition of directional spreading for all the angles.

Moreover, the distribution of wave heights and crests was investigated. Higher crests and heights were found for values of x/L>15 and for angles $\Delta\theta$=40°. The wave crests result is in agreement with the estimates made by Roberts (1983—see Fig. 4) for the maximum amplitudes of short-crested waves using Padé approximant for short-crested sea waves. In this numerical study, in fact, the maximum amplitude of waves

Table 1 Correlation coefficients between successive wave heights reported in previous studies (see Tables 3–4 and related references in Rodríguez and Guedes Soares (2001))

	R_{HH} (i,i+1)	R_{HH} (i,i+2)	R_{HH} (i,i+3)	R_{HH} (i,i+4)
Rye (1974)				
Wave growth	0.30			
Wave decay	0.20			
Total	0.24	≈0	≈0	
Dattatri et al. (1977)	0.236			
Arhan and Ezraty (1978)				
North Sea measur.	0.297	0.051	0.036	
Jonswap spectrum	0.298	0.113	<0.01	
P-M spectrum	0.163	0.043	<0.01	
Su et al. (1982)				
Wave growth	0.374	0.066	0	−0.021
Wave decay	0.34	0.07	0.021	0.013
Total	0.329	0.07	0.003	−0.006
Goda (1983)	0.649	0.351	0.178	0.07
Sobey (1996)				
P-M	0.31			
Mean Jonswap	0.45			
Sharp Jonswap	0.571			
Jayewardane (1987)				
Unimodal	0.17	0.091	0.055	
Bimodal	0.165	0.064	−0.041	
Rodríguez and Guedes Soares (2001)				
Swell-dominated sea (I)	0.311	0.064	0.01	−0.016
Swell-dominated sea (II)	0.520	0.135	0.015	0.012
Swell-dominated sea (III)	0.309	0.154	0.06	0.006
Wind-sea-dominated states (I)	0.549	0.189	0.05	−0.003
Wind-sea-dominated states (II)	0.419	0.148	−0.024	0.000
Wind-sea-dominated states (III)	0.621	0.217	0.061	0.009
Mixed wind-sea and swell systems with comparable energy (I)	0.204	0.02	0.012	−0.024
Mixed wind-sea and swell systems with comparable energy (II)	0.098	0.125	−0.011	0.011
Mixed wind-sea and swell systems with comparable energy (III)	0.194	0.059	0.05	−0.018
Pierson-Moskowitz	0.263	0.001	0.000	0.039
Rodríguez et al. (2000)-JONSWAP	0.444			
Wist et al. (2004)				
Draupner data	0.44	0.126	0.058	
Japan data	0.321	0.077	0.022	
Lab. data	0.516	0.170	0.079	
Present results				
$\Delta\theta$=10	0.475	0.073	−0.019	−0.020
$\Delta\theta$=20	0.513	0.140	0.017	−0.012
$\Delta\theta$=30	0.548	0.187	0.046	−0.009
$\Delta\theta$=40	0.574	0.195	0.029	−0.026
Unidirectional	0.518	0.108	−0.021	−0.041

increases between 10 and 30°, and for 40° we have a similar maximum wave height than 30°. For $x/L>22$, both wave crests and wave heights deviated from the Rayleigh and Socquet-Juglard second-order distribution, in coincidence of the maximum of the kurtosis along the wave tank. This is in agreement with the enhanced probability of rogue wave

Table 2 Correlation coefficients between successive wave crests and troughs

Crests				
$\Delta\theta=10$	0.372	0.043	−0.021	−0.020
$\Delta\theta=20$	0.411	0.109	0.008	−0.012
$\Delta\theta=30$	0.451	0.155	0.036	−0.010
$\Delta\theta=40$	0.487	0.160	0.021	−0.025
Unidirectional	0.425	0.078	−0.024	−0.039
Troughs				
$\Delta\theta=10$	0.395	0.057	−0.013	−0.011
$\Delta\theta=20$	0.428	0.112	0.015	−0.010
$\Delta\theta=30$	0.458	0.152	0.038	−0.008
$\Delta\theta=40$	0.489	0.159	0.020	−0.026
Unidirectional	0.442	0.087	−0.022	−0.035

appearance due to modulational instability and with wave tank observations in unidirectional sea state (Onorato et al. 2009b). Only in the case $\Delta\theta=10°$ the experimental data does not exceed the Rayleigh distribution for wave heights, suggesting that for $\Delta\theta>20°$ the nonlinearities become stronger.

We also observed the peak frequency decrease during the propagation of the wave train in the wave tank, obtaining similar results seen for unidirectional sea state in the same conditions of initial set of parameters (see Onorato et al. 2009b).

Onorato et al. (2010), studying the Coupled Nonlinear Schrodinger equations for crossing seas in deep water, discussed the behavior of the dispersive and the nonlinear coefficients as a function of $\Delta\theta$. They found in particular that the dispersion term of the CNLS, $-\alpha$, decreases with the angle and the ratio between cross-interaction and self-interaction decreases with the angle. The decreasing of the dispersive terms could be an explanation why the probability of freak waves increase with the crossing sea angle. However, for crossing sea angles $\Delta\theta<35.3°$, the dispersive and the nonlinear terms have the same sign, so this means that the system is focusing. At $\Delta\theta\approx35.3°$, the dispersive term become zero (see Fig. 1, Onorato et al. 2010) and a maximum of the kurtosis is expected. For $\Delta\theta>35.3°$, the dispersive term become negative and the system is no longer focusing. This should lead to a lower probability of rogue wave and a lower kurtosis. The present experiment, however, highlight that the angle with the highest probability for the establishment of a rogue sea, in the examined range, is $\Delta\theta=40°$ and for $\Delta\theta=10°$ the behavior of the waves are more Gaussian. Numerical simulations of a crossing sea using Potential Euler Equations (Toffoli et al. 2011) suggested that the highest probability of rogue waves in crossing seas is achieved in the range $40°<\Delta\theta<60°$, indicating $\Delta\theta=40°$ as the maxima of the kurtosis (Bitner-Gregersen and Toffoli 2014) and that the deviation from the Gaussian behavior occur for $\Delta\theta=20$–$30°$. Results also confirm that the kurtosis is a reliable indicator of an enhanced rogue wave probability in a crossing sea state.

The correlation coefficient between successive wave heights depends both on the crossing sea angle and on the spatial field of waves. In this case, higher values of wave correlation were found for $\Delta\theta=40°$: unidirectional values are exceeded by the values obtained for crossing angles greater than 20°. Similar results were obtained when analyzing correlation coefficients for wave crests and troughs. Wave heights correlation is also consistent with previous studies made in similar conditions both for laboratory studies and field measurements. Kimura (1980) discovered that the correlation coefficient between successive wave heights is linked with the wave group length. In particular, higher is this parameter, longer will be the wave group. This was experimentally confirmed by numerical simulations from a previous study in both unidirectional and crossing sea state (Rodríguez et al. 2000). Table 1 shows the comparison with values from previous studies. Results are comparable with numerical simulation carried out in JONSWAP conditions, while Pierson-Moskowitz spectra (both in crossing and in unidirectional) presents lower correlation coefficient, and, consequently, a shorter group length. A minimum for the successive wave height correlation was found for $\Delta\theta=10°$. The reason of this minimum is not totally clear, but the behavior of the correlation coefficient in the crossing sea is similar to the behavior of the kurtosis with $\Delta\theta$, suggesting that the reason for this could be linked to the ratio of the cross-interaction/self-interaction terms in CNLS equation highlighted in Onorato et al. (2010). Our results indicate a strong dependence between $\Delta\theta$ and correlation coefficient in the crossing sea state; however, the reason of this relation is not clear.

This study suggests the need to complete the analysis of the characteristics of the crossing sea states, considering the periods and spectral properties such as spectral bandwidth, the phase speeds of crests and troughs, and the degree of dependence between successive wave heights and periods. Moreover, other wave tank experiments are necessary to understand the behavior of wave heights in other different crossing sea angles $\Delta\theta>40°$, in particular for angles in the range of $40°<\Delta\theta<60°$, where some studies (Toffoli et al. 2011; Bitner-Gregersen and Toffoli 2014) predicted a higher probability of rogue waves, in order to investigate more deeply the dependence of rogue waves appearance probability and wave heights statistical variables and correlation in function of the crossing sea angle. Also, more experiment will be necessary to understand the role of directional spreading in a crossing sea and the dependence of rogue wave appearance with the variation of the directional spreading.

Acknowledgments We wish to acknowledge Ruari McIver, Alan McDonald, Mike Heath, and Miguel Onorato for their valuable

suggestions and always fruitful discussions. We wish also to acknowledge both of the anonymous reviewers that greatly improved the paper.

M.S. was supported by the EU, project EXTREME SEAS (SCP8-GA-2009-234175) and also by the Ministero dell'Istruzione, dell'Università e della Ricerca (Italy). A.D.S was supported by the University of Strathclyde, Scottish Environmental Protection Agency (SEPA) and Marine Scotland Science.

References

Akmediev N, Pelinovsky E (2010) Discussion and debate: rogue waves—towards a unifying concept? Eur Phys J 185:1–266

Arhan M, Ezraty R (1978) Statistical relations between successive wave heights. Ocean Acta 1:151–158

Benjamin BT, Feir JE (1967) The disintegration of wave train on deep water. J Fluid Mech 27:417–430

Bitner-Gregersen EM, Toffoli A (2014) Occurrence of rogue sea state and consequences for marine structures. Ocean Dyn 64:1457–1468

Bona JL, Saut JC (1993) Dispersive blowup of solutions of generalized Korteweg-de Vries equations. J Differ Equ 103(1):3–57

Cavaleri L, Bertotti L, Torrisi L, Bitner-Gregersen EM, Serio M, Onorato M (2012) Rogue Waves in crossing seas: the Louis Majesty accident. J Geophy Res 117(C11)

Cherneva Z, Guedes Soares C (2011) Evolution of wave properties during propagation in a ship towing tank and an offshore basin. Ocean Eng 38:2254–2261. doi:10.1016/j.oceaneng.2011.10.009

Christou M, Ewans KC (2011) Examining a comprehensive data set containing thousands of freak wave events. Part 2 – Analysis and findings. Proceedings of OMAE 2011 30th International Conference on Ocean, Offshore and Arctic Engineering. 19–24 June, 2011, Rotterdam, The Netherlands

Dattatri J, Raman H, Jothishankar N (1977) Wave groups: analysis of run and run length. In: Proceedings of the 6th Australasian Hydraulics Fluid Mechanics Conference, Adelaide

Donelan MA, Magnusson AK (2005) The role of meteorological focusing in generating rogue wave conditions. Proc. 14th Winther'Aha Huliko'a, Univ. Hawaii, USA

Donelan MA, Drennan WM, Magnusson AK (1996) Nonstationary analysis of the directional properties of propagating waves. J Phys Oceanogr 26:1901–1914

Dysthe K, Krogstad HE, Müller P (2008) Oceanic rogue waves. Annu Rev Fluid Mech 40:287–310. doi:10.1146/annurev.fluid.40.111406.102203

Galchenko A, Babanin AV, Chalikov D, Young IR, Hsu TW (2010) Modulational instabilities and breaking strength for deep-water wave groups. J Phys Oceanogr 40:2313–2324. doi:10.1175/2010JPO4405.1

Galchenko A, Babanin AV, Chalikov D, Young IR, Haus BK (2012) Influence of wind forcing on modulation and breaking of one-dimensional deep-water wave groups. J Phys Oceanogr 42:928–939. doi:10.1175/JPO-D-11-083.1

Goda Y (1983) Analysis of wave grouping and spectra of long-travelled swell. Rept Port Harb Res Inst 22:3–41

Gramstad O, Trulsen K (2007) Influence of crest and group length on the occurrence of freak waves. J Fluid Mech 582:463. doi:10.1017/S0022112007006507

Gramstad O, Trulsen K (2010) Can swell increase the number of freak waves in a wind sea? J Fluid Mech 650:57. doi:10.1017/S0022112009993491

Greenslade D (2001) A wave modelling study of the 1998 Sydney to Hobart yacht race. Aust Meteorol Mag 50:53–63

Gründlingh ML (1994) Evidence of surface wave enhancement in the southwest Indian Ocean from satellite altimetry. J Geophys Res Oceans (1978–2012) 99(C4):7917–7927

Guedes Soares C (1984) Representation of double-peaked sea wave spectra. Ocean Eng 11:185–207. doi:10.1016/0029-8018(84)90019-2

Guedes Soares C (1991) On the occurrence of double peaked wave spectra. Ocean Eng 18:167–171

Haver S (2004) A possible freak wave event measured at the Draupner jacket January 1 1995. Rogue Waves 2004:1–8

Janssen PAEM (2003) Nonlinear four-wave interactions and freak waves. J Phys Oceanogr 33:863–884

Janssen PAEM (2009) On some consequences of the canonical transformation in the Hamiltonian theory of water waves. J Fluid Mech 637:1–44. doi:10.1017/S0022112009008131

Jayewardane I (1987) Analysis of some bimodal spectra and the reproduction of these spectra in thelaboratory. In: Proceedings of the 2nd International Conference on Coastal and Port Engineering inDeveloping Countries, Beijing, China. COPEDEC, pp. 2046–2056

Kharif C, Pelinovsky E (2003) Physical mechanisms of the rogue wave phenomenon. Eur J Mech-B/Fluids 22(6):603–634

Kimura A (1980) Statistical properties of random wave groups. Coast Eng Proc 1:2955–2973

Komen G, Cavaleri L, Donelan M, Hasselmann K, Hasselmann H, Janssen PAEM (1994) Dynamics and modeling of ocean waves. Cambridge Univ. Press, Cambridge

Lavrenov IV (1998) The wave energy concentration at the Agulhas current off South Africa. Nat Hazards 17(2):117–127

Lavrenov IV (2003) Wind-waves in oceans: dynamics and numerical simulations. Springer

Longuet-Higgins MS (1952) On the statistical distribution of the heights of sea waves. J Marine Res 11:1245–1266

Longuet-Higgins MS (1963) The effect of non-linearities on statistical distributions in the theory of sea waves. J Fluid Mech 17:459–480

Longuet-Higgins MS (1984) Statistical properties of wave groups in a random sea state. Philos T Roy Soc A 312(1521):219–250

Magnusson AK, Donelan MA, Drennan WM (1999) On estimating extremes in an evolving wave field. Coast Eng 36(2):147–163

Mori N, Janssen PAEM (2006) On kurtosis and occurrence probability of freak waves. J Phys Oceanogr 36:1471–1483

Mori M, Onorato M, Janssen PAEM, Osborne AR, Serio M (2007) On the extreme statistics of long-crested deep water waves: theory and experiments. J Geophys Res 112(C09011). doi:10.1029/2006JC004024

Mori N, Onorato M, Janssen PAEM (2011) On the estimation of the kurtosis in directional sea states for freak wave forecasting. J Phys Oceanogr 41:1484–1497. doi:10.1175/2011JPO4542.1

Muller P, Garrett C, Osborne AR (2005) Rogue waves. Oceanography 18(3):66

Nikolkina I, Didenkulova I (2011) Catalogue of rogue waves reported in media in 2006–2010. Natural Hazards 1–18

Onorato M, Osborne AR, Serio M, Bertone S (2001) Freak waves in random oceanic sea states. Phys Rev Lett 86:5831

Onorato M, Osborne AR, Serio M (2002) Extreme wave events in directional, random oceanic sea state. Phys Fluids 14:L25–L28

Onorato M, Osborne AR, Serio M, Cavaleri L (2005) Modulational instability and non-Gaussian statistics in experimental random water-wave trains. Phys Fluids 17(7):078101

Onorato M, Osborne AR, Serio M (2006) Modulational instability in crossing sea states: a possible mechanism for the formation of freak waves. Phys Rev Lett 96(1):014503

Onorato M, Waseda T, Toffoli A, Cavaleri L, Gramstadt O, Janssen PAEM, Kinoshita T, Monbaliu J, Mori N, Osborne AR, Serio M, Stansberg CT, Tamura H, Trulsen K (2009a) Statistical properties of directional ocean waves: the role of modulational

instability in the formation of extreme events. Phys Rev Lett 102(11):114502

Onorato M, Cavaleri L, Fouques S, Gramstad O, Janssen PAEM, Monbaliu J, Osborne AR, Pakozdi C, Serio M, Stansberg C, Toffoli A, Trulsen K (2009b) Statistical properties of mechanically generated surface gravity waves: a laboratory experiment in a 3d wave basin. J Fluid Mech 627:235–257

Onorato M, Proment D, Toffoli A (2010) Freak waves in crossing seas. Eur Phys J 185:45–55. doi:10.1140/epjst/e2010-01237-8

Onorato M, Residori S, Bortolozzo U, Montina A, Arecchi FT (2013) Rogue waves and their generating mechanisms in different physical contexts. Phys Rep. doi:10.1016/j.physrep.2013.03.001

Pelinovsky E, Talipova T, Kurkin A, Kharif C (2001) Nonlinear mechanism of tsunami wave generation by atmospheric disturbances. Nat Hazards Earth Syst Sci 1(4):243–250

Roberts AJ (1983) Highly nonlinear short-crested water waves. J Fluid Mech 135:301–321. doi:10.1017/S0022112083003092

Rodríguez GR, Guedes Soares C (2001) Correlation between successive wave heights and periods in mixed sea states. Ocean Eng 28:1009–1030

Rodríguez GR, Guedes Soares C, Ferrer L (2000) Wave group statistics of numerically simulated mixed sea states. J Offshore Mech Arct Eng 122:282–288

Rye H (1974) Wave group formation among storm waves. In: Coastal Eng. Proceedings

Sobey RJ (1996) Correlation between individual waves in a real sea state. Coast Eng 27:223–242. doi:10.1016/0378-3839(96)00010-5

Socquet-Juglard H, Dysthe K, Trulsen K, Krogstad HE, Liu J (2005) Distribution of surface gravity waves during spectral changes. J Fluid Mech 542:195–216

Su MY, Bergin MT, Bales SL (1982) Characteristics of wave groups in storm seas. In: Proceedings Ocean Structural Dynamics Symposium

Tayfun MA (1980) Narrow-band nonlinear sea waves. J Geophys Res 85:1548–1552

Toffoli A, Onorato M, Monbaliu J (2006) Wave statistics in unimodal and bimodal seas from a second-order model. Eur J Mech B/Fluids 25:649–661. doi:10.1016/j.euromechflu.2006.01.003

Toffoli A, Bitner-Gregersen EM, Osborne AR, Serio M, Monbaliu J, Onorato M (2011) Extreme waves in random crossing seas: Laboratory experiments and numerical simulations. Geoph Res Lett 38. doi:10.1029/2011GL046827

White BS, Fornberg B (1998) On the chance of freak waves at sea. J Fluid Mech 355:113–138

Wist HT, Myrhaug D, Rue H (2004) Statistical properties of successive wave heights and successive wave periods. Appl Ocean Res 26:114–136. doi:10.1016/j.apor.2005.01.002

Young IR (1995) The determination of confidence limits associated with estimates of spectral peak frequency. Ocean Eng 22(7):669–686

Zakharov VE, Ostrovsky LA (2009) Modulation instability: the beginning. Phys D Nonlinear Phenom 238:540–548. doi:10.1016/j.physd.2008.12.002

Zakharov VE, Dyachenko AI, Prokofiev AO (2006) Freak waves as nonlinear stage of Stokes wave modulation instability. Eur J Mech B/Fluids 25(5):677–692